

# DIRECT NUMERICAL SIMULATION FOR VERY LARGE-SCALE MOTIONS IN A TURBULENT BOUNDARY LAYER

Jae Hwa Lee and Hyung Jin Sung\*

Department of Mechanical Engineering, KAIST  
291 Daehak-ro, Yuseong-gu, Daejeon, 305-701, Korea  
Jhlee06@kaist.ac.kr, hjsung@kaist.ac.kr

## ABSTRACT

Direct numerical simulation (DNS) of a turbulent boundary layer (TBL) was performed to investigate the spatially coherent structures associated with very large-scale motions (VLSMs). The Reynolds number was varied in the range  $Re_\delta=570\sim 2560$ . Inspection of the three-dimensional instantaneous fields showed that groups of hairpin vortices are coherently arranged in the streamwise direction and that these groups create significantly elongated low- and high-momentum regions with large amounts of Reynolds shear stress. Adjacent packet-type structures combine to form the VLSMs; this formation process is attributed to continuous stretching of the hairpins coupled with lifting-up and backward curling of the vortices. We employed the modified feature extraction algorithm developed by Ganapathisubramani *et al.* (2003) to identify the properties of the VLSMs of hairpin vortices. In the log layer, patches with the length greater than  $3\sim 4\delta$  account for more than 40% of all the patches and these VLSMs contribute approximately 45% of the total Reynolds shear stress included in all the patches.

## INTRODUCTION

Many experimental and numerical studies have shown that large-scale organized structures that tend to align in the streamwise direction into coherent groups in the logarithmic layer play a crucial role in the transport of turbulent shear flow. These structures are known as hairpin vortex packets and have streamwise extents on the order of  $2\sim 3\delta$ , where  $\delta$  is the thickness of the boundary layer (Adrian *et al.* 2000; Adrian & Tomkins 2003; Ganapathisubramani *et al.* 2003). In addition, recent experimental and numerical results have revealed the existence of a new type of motion (with sizes in the range  $10\sim 50\delta$ ) with a larger scale than the large-scale motions (LSMs) corresponding to bulges or hairpin packets (Kim & Adrian 1999; Guala *et al.* 2006; Balakumar & Adrian 2007). Adrian (2007) and Marusic *et al.* (2010) have provided an excellent review of these interesting structures including the LSMs. Kim & Adrian (1999) examined pre-multiplied spectra for a turbulent pipe flow at  $y^+=132$  and interpreted their shapes as indicating a bi-modal distribution in which the wavelengths at which the maxima occur represent VLSMs and LSMs. Guala *et al.* (2006) and Balakumar & Adrian (2007) investigated the pre-multiplied power spectra of velocity fluctuations and determined criteria for distinguishing between VLSMs and LSMs in turbulent pipe flows, channel flows, and boundary layers. They found that the maximum streamwise extent of LSMs is about  $3\delta$ , and that the boundary that distinguishes VLSMs

from LSMs and smaller motions is  $k_x\delta=2$  due to the crossover in the co-spectra of  $u$  and  $v$ .

However, the general form of VLSMs in turbulent flows is not certain due to the experimental and computational difficulties in the study of larger wavelengths, such as the limited spatial region ( $2\sim 3\delta$ ) of PIV due to the constraints of the field of view of the camera, the difficulties in producing extensive light sheets, and the need for long computational boxes to include VLSMs that occur at high Reynolds numbers. To address these problems, Hutchins & Marusic (2007) performed experiments with a spanwise rake of 10 hot-wires in the TBL. By using Taylor's approximation, which converts temporal experimental measurements into a spatial domain, they found evidence of very long meandering features that had typical streamwise extents of greater than  $20\delta$  in the instantaneous flow fields. By comparing typical PIV images with the very long meandering rake signal, Hutchins & Marusic (2007) showed that the stripes observed in the log region of the rake data are similar to those observed previously in PIV data. They conjectured that these motions in turbulent pipe flow can be explained by what Kim & Adrian (1999) referred to as VLSMs that arise from the coherent alignment of LSMs associated with hairpin packets.

In the present study, DNSs of a TBL at moderate Reynolds numbers were conducted to investigate the spatially coherent structures associated with VLSMs. A fully three-dimensional understanding of these flow structures remains elusive, and several issues are unresolved: *What* are the typical structures of VLSMs and their properties? And *how* are they created in flow fields? In the following section, these questions are addressed by considering the time-resolved instantaneous three-dimensional flow fields. In particular, the modified feature extraction algorithm developed by Ganapathisubramani *et al.* (2003) was adopted to identify the properties of the VLSMs, such as their frequency and contribution to the Reynolds shear stress in the flow fields.

## NUMERICAL METHOD

For an incompressible flow, the nondimensional governing equations are

$$\frac{\partial u_i}{\partial t} + \frac{\partial u_i u_j}{\partial x_j} = -\frac{\partial p}{\partial x_i} + \frac{1}{\text{Re}} \frac{\partial^2 u_i}{\partial x_j \partial x_j} + f_i \quad (1)$$

$$\frac{\partial u_i}{\partial x_i} = 0 \quad (2)$$

where  $x_i$  are the Cartesian coordinates and  $u_i$  are the corresponding velocity components. All variables are nondimensionalized by the free-stream velocity ( $U_\infty$ ) and momentum thickness at the inlet ( $\theta_{in}$ ), and  $Re$  is the Reynolds number. The governing equations are integrated in time by using the fractional step method with the implicit velocity decoupling procedure proposed by Kim *et al.* (2002). In the block LU decomposition, both the velocity-pressure decoupling and any additional decoupling of the intermediate velocity components were achieved through approximate factorization. In this approach, the terms are first discretized in time by using the Crank-Nicholson method, and then the coupled velocity components are solved without iteration. All terms were resolved by using a second-order central difference scheme in space with a staggered mesh.

The notational convention adopted is that  $x$ ,  $y$ , and  $z$  denote the streamwise, vertical, and spanwise coordinates, respectively, and that  $u$ ,  $v$ , and  $w$  denote the streamwise, wall-normal, and spanwise components of the velocity fluctuation, respectively. The no-slip boundary condition was imposed at the solid wall, and the boundary conditions on the top surface of the computational domain were  $u = U_\infty$  and  $\partial v/\partial y = \partial w/\partial y = 0$ . Periodic boundary conditions were applied in the spanwise direction. Since the boundary layer is developing spatially in the downstream direction, it is necessary to use non-periodic boundary conditions in the streamwise direction. To overcome the difficulties associated with these boundary conditions, and to avoid the simulation of the laminar and transitional regions arising near a leading-edge, an auxiliary simulation based on the method of Lund *et al.* (1998) was carried out to acquire time-dependent turbulent inflow data with a sufficiently long streamwise domain, because the use of Lund's original method in a short streamwise domain can produce numerical periodicity in the flow fields. At the exit, the convective boundary condition was specified as  $(\partial u/\partial t) + c(\partial u/\partial x) = 0$ , where  $c$  is the local bulk velocity. Further details of the numerical method can be found in the paper of Lee & Sung (2011).

### TIME-RESOLVED INSTANTANEOUS FIELDS

In this section, we address the question of the streamwise scale of the packets that create VLSMs in the flow field. The idea that small scales organize coherently to create larger scales is interesting and has received increasing support over the past few decades. The hairpin packet model for the effects of hairpin vortices offers an explanation for the most fundamental features of the logarithmic layer, such as bursting processes and quasi-streamwise vortices. Adrian *et al.* (2000) described an idealized conceptual model based on the hairpin packet paradigm, and showed how it explains most features of the coherent structures in the outer region. In contrast, Kim & Adrian (1999) suggested a simple hypothesis that does not require the recognition of VLSMs as a new type of turbulent motion. They conjectured that VLSMs may be alignments of spatial coherence between hairpin packets; turbulent flows are abundantly populated with packets. Unfortunately, however, little is known about the formation of VLSMs and

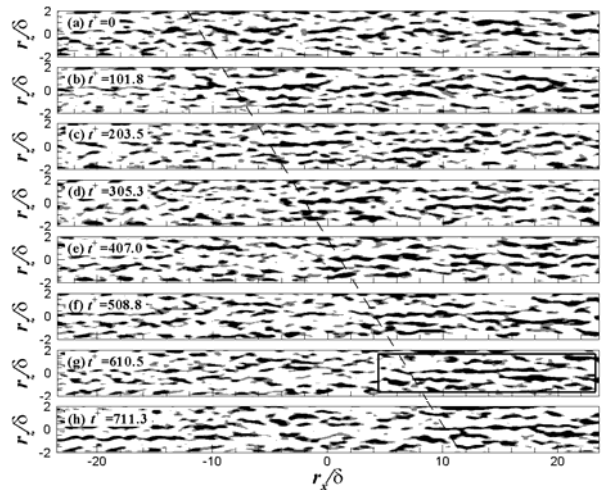


Figure 1: Time-resolved instantaneous fields in the  $xz$  plane. The black and grey levels indicate the  $-1.0$  and  $-0.5 u^+$  contours.

how they are created in the flow field. The objective of the present study was to obtain spatial information about the formation of VLSMs from packets by examining the time-resolved instantaneous flow fields.

The autogeneration mechanisms mean that the hairpins combine to create packets that are long in the streamwise direction by continually spawning new hairpins. As they grow, the packets become longer and larger in the streamwise and spanwise directions, and are eventually probably broken up into smaller scale structures or merge with adjacent packets. Figure 1 shows the time evolution of the entire flow field in the  $xz$  plane with a time interval  $t^+ = 101.8$ . The black and gray levels depict the  $-1.0$  and  $-0.5$  streamwise velocity fluctuations respectively normalized by the friction velocity and the wall-normal height is  $y/\delta = 0.21$ . Since the real turbulence flow pattern is complex and it is hard to discern the obvious features of scale growth in the full domain, the Gaussian filter was employed in the present study. The dashed line was added to show the growth of the VLSM. It is clear that the VLSM at  $t^+ = 711.3$  in the range  $8 < r_x/\delta < 24$  originate in several packet motions present at  $t^+ = 0$ . These packets that are still growing in the streamwise direction interact with adjacent packets in the streamwise direction and the merging packets result in the streamwise-aligned VLSM at  $t^+ = 101.8$ . The VLSM is also growing continuously both in the streamwise and spanwise directions. After  $t^+ = 407.0$ , however, although the streamwise growth of the VLSM occurs, the spanwise length becomes thinner.

To show the streamwise scale growth, magnified views of figure 1 with small temporal variation were examined through the  $xz$  and  $xy$  planes in figures 2 and 3. Figure 2(a) shows two adjacent low-momentum regions induced by the hairpin packets in the range  $-14.7 < r_x/\delta < -11.7$  and  $-11.2 < r_x/\delta < -6.5$ . These regions are traveling with similar convection velocities in the  $xz$  plane. As they move downstream, the low-momentum regions merge in the streamwise direction, resulting in a longer structure on the streamwise scale. Figure 3 shows the associated flow features in the  $xy$  plane. The contours of the streamwise velocities  $U = 0.6, 0.7, \text{ and } 0.9U_\infty$  are shown and the data were extracted along the streamwise direction at  $r_z/\delta = 0.2$

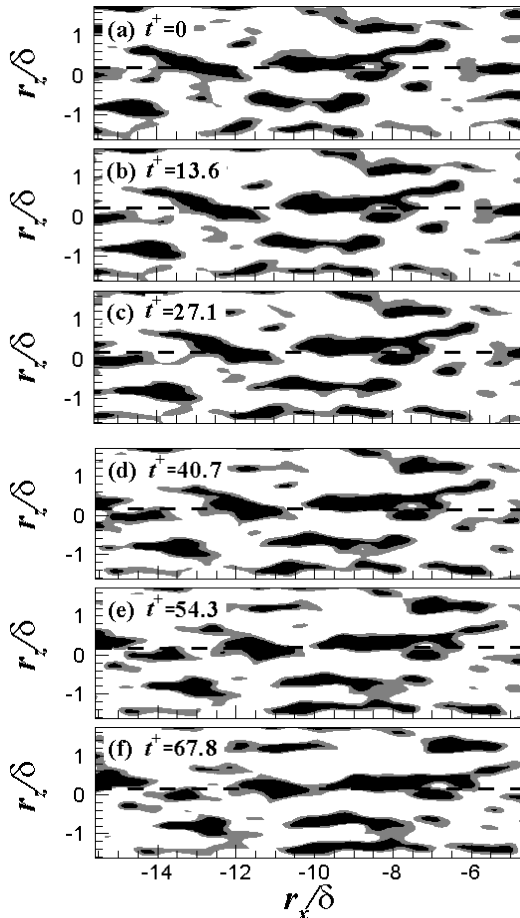


Figure 2: Time-resolved instantaneous fields in the  $xz$  plane. The black and grey levels indicate the  $-1.0$  and  $-0.5 u^+$  contours.

from figure 2, as depicted by the dashed lines in figure 2. There are zones of multiple uniform momentums that are created by successive hairpin vortices and larger, presumably older packets including the small presumably young packets lying close to the wall, although the swirling strengths and velocity vectors are omitted from the figure to show the dynamics of the hairpin packets. Based on the contour  $U=0.7U_\infty$ , there are two packets of hairpins containing uniform momentum zones labeled IA and IB at  $t^+=13.6$  in the regions  $-14 < r_x/\delta < -11.5$  and  $-11.5 < r_x/\delta < -8.5$ . These are inclined at angles of  $10\sim 15^\circ$  in an almost linear fashion. Note that the flow patterns of these aligned packets are consistent with the observations of Adrian *et al.* (2000); see e.g., figure 19. If we search for low-momentum regions along the streamwise slice at  $y/\delta=0.21$  (dashed lines), results consistent with those in the  $xz$  plane are found.

As can be seen in this figure, these packets are growing continuously in the downstream direction and the part of the upstream packet further away from the wall (the hairpin head or arch) experiences the higher mean flow velocity. This part flows downstream faster than the lower-lying parts, which causes the vortex to lift away from the wall with a still higher mean velocity, and results in still greater stretching and rolling-up in the upper part of the upstream packet. Consequently, this packet merges with the adjacent packet in the downstream to form a VLSM with a shallow

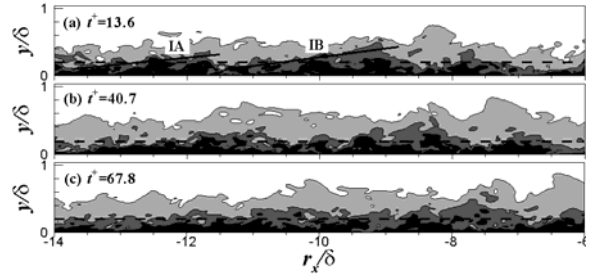


Figure 3: Evidence of streamwise scale growth in the  $xy$  plane. The contours are the streamwise velocities,  $U=0.6, 0.7$  and  $0.9U_\infty$  and the data are extracted along the streamwise direction at  $r_z/\delta=0.2$  in figure 2. The dashed lines are depicted for the  $xz$  plane in figure 2.

angle to the streamwise direction at  $t^+=67.8$ . These processes are consistent with the hairpin structure dynamics proposed by Zhou *et al.* (1999). They found that quasi-streamwise vortices lift up away from the wall due to the vortex leg and that the hairpin vortices are influenced by the mean shear, which stretches and intensifies the vortices in the downstream direction. These findings indicate that one consequence of a balance between the lifting-up and backward curling of vortices due to the vortex-induced motion of the hairpin legs and the vortex stretching due to the mean shear is the merging of adjacent hairpin packets and thus the formation of a VLSM in the logarithmic layer. However, this merging process does not occur frequently so VLSMs are found less often than packets in flow fields.

As discussed in the previous section, hairpins can spawn new downstream hairpins and create packets that are long in the streamwise direction. As they grow, the packets simultaneously become larger in the wall-normal and spanwise directions. This growth is associated with the growth of individual hairpins, but streamwise growth also depends on the coherent alignment of successive hairpins (Zhou *et al.* 1999; Adrian *et al.* 2000). The growth of hairpin packets moving in the streamwise direction can be explained as a consequence of a balance between the mean shear stretching of the hairpin head in the streamwise direction and the effects of self-induction, which result in the curling up of quasi-streamwise vortices and the lifting of the head away from the wall (Zhou *et al.* 1999). These processes are consistent with Townsend's attached eddy hypothesis, which suggests that the sizes of eddies are proportional to the distance from the wall. This scale growth occurs continuously in the wall-normal and spanwise directions, which implies that there is likely to be an interaction between hairpin vortices in the spanwise direction as they move downstream. Tomkins & Adrian (2003) analyzed the merging of vortex packets in a mechanism of spanwise scale growth that is similar to that of Adrian *et al.* (2001).

The spanwise scale growth occurs between VLSMs, as shown in figure 4. The vector fields with patches of  $\lambda_{ci}\omega_y/|\omega_y|$  are depicted in figure 4(a) for the  $xz$  plane and the time is set to  $t^+=0$  for convenience. At  $t^+=0$ , two elongated low-momentum regions induced by the alignment of the hairpin vortices are travelling parallel to the streamwise direction. These motions appear to have comparable size in the spanwise direction and create low-high-low fluid

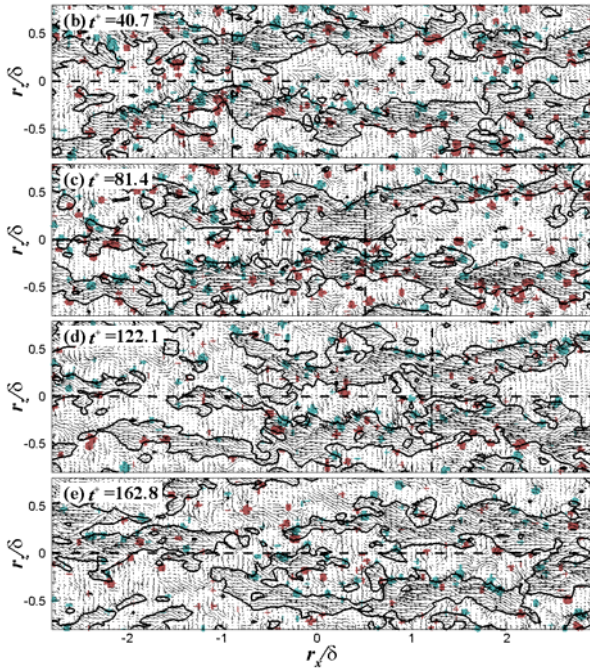


Figure 4: Evidence of spanwise scale growth through packet merging in the  $xz$  plane. Velocity vectors and patches of  $\lambda_{ci}\omega_y/|\omega_y|$  at (a)  $t^+=0$ ; (b)  $t^+=40.7$ ; (c)  $t^+=81.4$ ; (d)  $t^+=122.1$ ; (e)  $t^+=162.8$ .  $U_c=0.7U_\infty$ ,  $y/\delta=0.19$ . The dashed lines are depicted for the  $yz$  plane in figure 5.

patterns. When the interaction of the VLSMs occurs at a certain downstream position where the distance between the vortices becomes small, the low-momentum regions are gradually merging in the spanwise direction and eventually combined in the range  $1 < r_x/\delta < 2$  at  $t^+=122.1$ . The merged structure has roughly double the spanwise scale, which induces a weaker backward flow according to the Biot-Savart law. In addition, a stagnation point is present at the interface between the upstream and downstream packets.

Figure 5 illustrates the flow features in the  $yz$  plane at the four streamwise locations  $r_x/\delta=-1.8, -0.9, 0.5$ , and  $1.2$  shown in figure 4. Note that these data were extracted at the same time. There are two low-momentum regions elongated in the wall-normal direction and these were created by the induction of the legs of the hairpin packets, as shown in figure 5(a) at  $t^+=0$ . The inner sides of these momentum zones gradually merge due to the interaction between them at  $t^+=81.4$ , which indicates that the inner legs of the hairpins that have the opposite swirl are annihilated and that only the outer legs of the larger hairpins eventually survive along the wall-normal direction. However, the size in the wall-normal direction is comparable to that of the initial vortex. These conclusions are similar to the features of the proposals of Tomkins & Adrian (2003). They assumed a complete annihilation of the legs of hairpin-type structures, which results in a new hairpin of approximately double the width of each of the original individual hairpins. After merging, the new hairpin is expected to have an effect on the evolution of the other structures. These results from the time sequence of the instantaneous fields in the  $xz$  and  $yz$  planes demonstrate that the spanwise scale growth due to merging occurs continuously in time and that the spanwise scale increases rapidly to twice the original width of the packets,

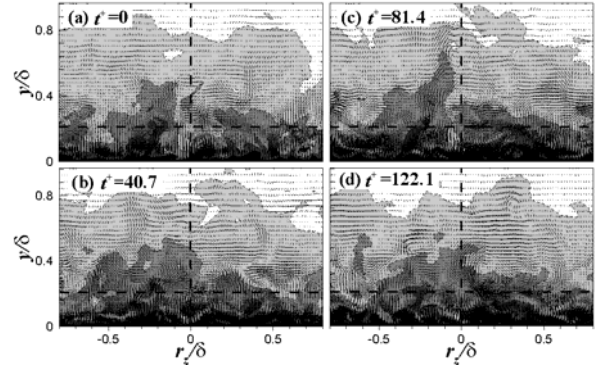


Figure 5: Time evolution of the merging structure in the  $yz$  plane at the streamwise locations  $-1.8, -0.9, 0.5$  and  $1.2\delta$  shown in figure 4. Velocity vectors with streamwise velocities,  $U=0.3, 0.5, 0.7$  and  $0.9U_\infty$  at (a)  $t^+=0$ ; (b)  $t^+=40.7$ ; (c)  $t^+=81.4$ ; (d)  $t^+=122.1$ . The dashed lines are depicted for the  $xz$  in figures 4.

which indicates that this mechanism for spanwise merging is an essential process in turbulent flows.

## PROPERTIES OF THE VERY-LARGE SCALE MOTIONS

The properties of the VLSMs discussed in the following section were estimated statistically from the instantaneous fields using the feature extraction algorithm originally developed by Ganapathisubramani *et al.* (2003). We classified the Reynolds shear stress into the second- and fourth-quadrant components that are associated with very long negative and positive packets respectively and examined their properties. The algorithm is as follows. *i*) Zones of the second-quadrant of Reynolds shear stress  $> 2\sigma_{uv}^+$  are identified, where  $\sigma_{uv}^+$  is the r.m.s. of the Reynolds shear stress. *ii*) If the zones found in *i*) are observed between positive and negative swirling strength  $> |1.5\sigma_{\lambda_{ci}}^+|$ , where  $\sigma_{\lambda_{ci}}^+$  is the r.m.s. of the swirling strength, one of the points in the center regions are defined as seed point at each location. Note that since all points found in each zone are included in one packet motion, so it is necessary to select a representative point, although it does not matter which point is chosen. *iii*) Based on the seed point, we identified the connected low-momentum regions (negative streamwise velocity fluctuations) in the flow fields.

After the calculations for the Q2 event, we applied the same procedures for the Q4 event with high-momentum regions (positive streamwise velocity fluctuations). However, since the estimated results for the Q4 event are almost the same as those for the Q2 event, only the results for the Q2 event are shown in the present study. Such results can be expected, because the inclination of hairpin vortices with respect to the wall is such that the region outside of the legs/neck should induce the Q4 events and the counter-rotating hairpin vortices inducing the low-speed flow also create the high-speed flows on either side of the low-momentum regions, as shown in the  $xz$  plane (Adrian *et al.* 2000; Ganapathisubramani *et al.* 2003).

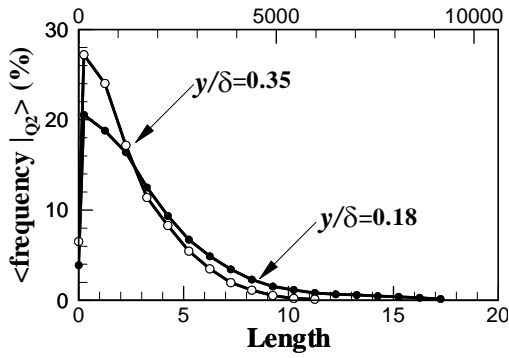


Figure 6: Length statistics for the patches found by the feature extraction algorithm (Q2 event) at  $y/\delta=0.18$  and  $0.35$ . The length is normalized by the inner (top) and outer (bottom) units.

Figure 6 shows the length distribution of the identified structures, which was obtained with the feature extraction algorithm at  $y/\delta=0.18$  and  $0.35$ . The ordinate in figure 6 is the ratio of the number of the patches found in each length to the total number of detected patches. Note that the length for the VLSMs is defined as greater than  $3\sim 4\delta$  in the present study, based on the criteria of Guala *et al.* (2006) and Balakumar & Adrian (2007). In the log layer, the peak occurs at less than approximately  $0.25\delta$  ( $\sim 150$  in wall units), which indicates that the predominant structure is a single hairpin vortex. This conclusion is consistent with that of Ganapathisubramani *et al.* (2003). They showed that the peak occurs near 100 wall units. As the length increases, the frequency of the occurrence of patches decreases monotonically. The long tail of the curve is due to the presence of elongated streamwise-aligned structures in the log layer, although the number of VLSMs with lengths larger than  $10\delta$  is small. The results show that the alignment of successive hairpin vortices into packets is more frequently happened than the alignment of hairpin packets to form VLSMs. However, the VLSMs exceeding  $3\sim 4\delta$  in length account for more than 40% of all the patches identified by the extraction scheme. The maximum length of the VLSMs found by the identification algorithm is approximately  $\sim 18\delta$  in the streamwise direction, a result that is comparable to that of Hutchins & Marusic (2007). They found regions of very long meandering positive and negative streamwise velocity fluctuations exceeding  $20\delta$ . Simple calculations show that the mean streamwise length of the patches with various length scales is  $5.87\delta$ ; this value is similar to that indicated by the two-point correlations of the present studies. Individual hairpin packets (less than  $2\sim 3\delta$ ) are more frequently observed in the wake region than in the log layer, and the highly elongated streamwise coherence of the structures found in the logarithmic layer decreases far from the wall.

The length contributions to the total Reynolds shear stress are shown in figure 7. The values in figure 7 were computed as the ratio of the total second-quadrant Reynolds shear stress associated with all patches included in a certain length to the sum of the second-quadrant Reynolds shear stress for all patches identified by the feature extraction algorithm. The maximum contribution to the Reynolds

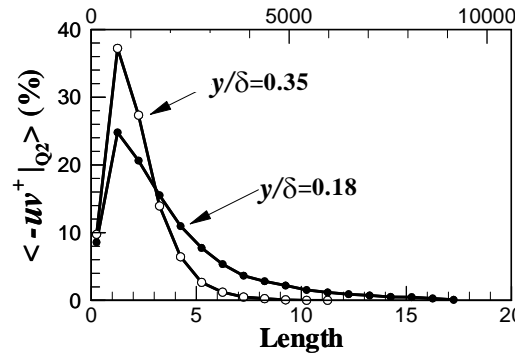


Figure 7: The contribution to the total second-quadrant Reynolds shear stress identified by the feature extraction algorithm (Q2 event) as functions of the length. The length is normalized by the inner (top) and outer (bottom) units.

shear stress arises at  $1\sim 2\delta$  in the log and wake regions (Ganapathisubramani *et al.* 2003), and the LSMs and VLSMs with lengths greater than  $\sim 1\delta$  contribute more significantly to the Reynolds shear stress than the smaller single hairpin vortices. Although the frequency is maximum at approximately  $\sim 0.5\delta$ , the streamwise-aligned packets contribute most of the Reynolds shear stress. The VLSMs ( $>3\sim 4\delta$ ) related to the Q2 events in the log layer contribute more than approximately 45% of all the second-quadrant Reynolds shear stress identified by the feature extraction algorithm and since the results for the Q4 event are the same as for the Q2 event, it can be inferred that the VLSMs in the log layer contribute more than 45% of the Reynolds shear stress identified by the identification algorithm. These findings demonstrate the importance of the VLSMs to the Reynolds shear stress in wall-bounded turbulent flows. When the total Reynolds shear stress identified by the extraction algorithm is divided by the global sum of all Reynolds shear stress in all vector fields, we find that the contribution of the log layer is approximately 20%. This value is similar to that reported by Ganapathisubramani *et al.* (2003).

## CONCLUSIONS

We carried out the DNS of a TBL to investigate the spatial features and properties of its VLSMs. The Reynolds number based on the momentum thickness ( $\theta_m$ ) and the free-stream velocity ( $U_\infty$ ) was varied in the range  $Re_\theta=570\sim 2560$ . We inspected the time-resolved instantaneous flow fields to investigate the streamwise and spanwise scale growth of the hairpin vortex packets. As the packets grow in the streamwise direction, they interact with adjacent packets and then merge with them, resulting in longer structures in the streamwise direction. Two adjacent packets of hairpins interacting with each other were observed. These packets grew continuously in the downstream and upstream directions, and packets further away from the wall (hairpin heads or arches) exhibited higher mean velocities. This upstream packet convected downstream faster than its lower-lying parts, which caused the vortex to lift away from the wall at a still higher mean velocity and resulted in still greater stretching and rolling of

the hairpin head. As a result, this packet merged with the upstream part of the adjacent downstream packet to form a VLSM with a shallow angle with respect to the streamwise direction. These observations show how large streamwise scales of packets merge to create VLSMs in flow fields. However, although this process occurs in many instantaneous fields, in reality an enormous range of relative flow configurations not examined in the present study can result in merging. The present findings describe only one of the possible mechanisms for VLSM formation through merging, and hence more thorough analysis of other merging mechanisms is required.

In addition, to provide additional information about the mechanism of spanwise scale growth, the three-dimensional characteristics of the merging process were determined by examining the time evolution of the instantaneous fields. Unmerged packets with comparable size in the spanwise direction were found upstream; these two adjacent packets moved in parallel before merging and then these packets combined to create the downstream, merged packet with weaker backflows and double the spanwise width. The inner sides of the two elongated low-momentum regions in the wall-normal direction, which feature swirling motions with opposite signs, are annihilated and eventually only the outer sides survive as part of the larger structure in the spanwise direction. These results support the mechanism for spanwise scale growth of merging.

The frequency and the contribution to the Reynolds shear stress of the VLSMs were estimated via a feature extraction algorithm that was developed to search for regions of uniform momentum enveloped by cores of swirling motions of opposite sign with significant Reynolds shear stress. The identified patches with lengths greater than  $3\text{--}4\delta$  account for more than 40% of all the patches and these VLSMs contribute approximately 45% of the total Reynolds shear stress due to all patches, which indicates the importance of VLSMs to the Reynolds shear stress as well as to turbulence production and the transport of momentum in the logarithmic layer.

## ACKNOWLEDGEMENT

This work was supported by the Creative Research Initiatives (No. 2011-0000423) of the National Research Foundation of Korea.

## REFERENCES

- Adrian, R. J., 2007, "Hairpin vortex organization in wall turbulence," *Phys. Fluids* 19, 041301.
- Adrian, R. J., Balachander, S., & Liu, Z. -C., 2001, "Spanwise growth of vortex structure in wall turbulence," *KSME Intl J.* 15, 1741-1749.
- Adrian, R. J., Meinhart, C. D., and Tomkins, C. D., 2000, "Vortex organization in the outer region of the turbulent boundary layer," *J. Fluid Mech* 422, 1-54.
- Balakumar, B. J., & Adrian, R. J., 2007, "Large- and very-large-scale motions in channel and boundary-layer flows," *Phil. Trans. R Soc. Lond. A* 365, 665-681.
- Ganapathisubramani, B., Longmire, E. K., & Marusic, I., 2003, "Characteristics of vortex packets in turbulent boundary layers," *J. Fluid Mech* 478, 35-46.

Guala, M., Hommema, S. E., & Adrian, R. J., 2006, "Large-scale and very-large-scale motions in turbulent pipe flow," *J. Fluid Mech* 554, 521-542.

Hutchins, N., & Marusic, I., 2007, "Evidence of very long meandering features in the logarithmic region of turbulent boundary layers," *J. Fluid Mech* 579, 1-28.

Kim, K., Baek, S. -J., and Sung, H. J., 2002, "An implicit velocity decoupling procedure for the incompressible Navier-Stokes equations," *Intl J Numer Meth Fluids* 38, 125-138.

Kim, K. C., & Adrian, R. J., 1999, "Very large-scale motion in the outer layer," *Phys. Fluids* 11, 417-422.

Lee, J. H., & Sung, H. J., 2011, "Direct numerical simulation of a turbulent boundary layer up to  $Re_{\theta} = 2500$ ," *Intl J. Heat Fluid Flow* 32, 1-10.

Lund, T. S., Wu, X., & Squires, K. D., 1998, "Generation of turbulent inflow data for spatially-developing boundary layer simulation," *J. Comput. Phys* 140, 233-258.

Marusic, I., Mckeon, B. J., Monkewitz, P. A., Nagib, H. M., Smits, A. J., & Sreenivasan, K. R., 2010, "Wall-bounded turbulent flows at high Reynolds numbers: Recent advances and key issues," *Phys. Fluids* 22, 065103.

Tomkins, C. D., & Adrian, R. J., 2003, "Spanwise structure and scale growth in turbulent boundary layers," *J. Fluid Mech* 490, 37-74.

Zhou, J., Adrian, R. J., Balachandar, S., & Kendall, T. M., 1999, "Mechanisms for generating coherent packets of hairpin vortices," *J. Fluid Mech* 387, 353-396.